ELSEVIER

International Journal of Mass Spectrometry 220 (2002) 53–67

International Journal of Mass Spectrometry

www.elsevier.com/locate/ijms

Catalysis models for the enolization of the acetaldehyde radical cation

Maciej Haranczyk [a], Peter C. Burgers [b], Paul J.A. Ruttink [c,*]

[a] *Department of Chemistry, The University of Gdansk, ul. Sobieskiego 18, 80-952 Gdansk, Poland*
[b] *Hercules European Research Center BV, Nijverheidsweg 60, 3771 ME Barneveld, The Netherlands*
[c] *Theoretical Chemistry Group, Department of Chemistry, Utrecht University, 3584 CH Utrecht, The Netherlands*

Received 8 May 2002; accepted 4 July 2002

Abstract

The catalysis of the enolization of the prototype aldehyde radical cation in the gas phase using methanol or acetaldehyde as the catalyst was studied theoretically. For the computations the CBS-Q model was used, in combination with RHF/DZP optimized geometries. Various reaction path models were tested, including the proton-transport catalysis (PTC) model, the Spectator model and the Quid pro Quo (QpQ) model. For the latter model there are several possibilities, depending on the choice made for the catalyst hydrogen to be exchanged. For some reaction steps no transition states exist. Instead, there are intersections of two potential energy surfaces corresponding to different localizations of the radical site in the ion–molecule complex. For acetaldehyde both the PTC and QpQ (all variants) models are shown to be feasible. However, the barrier heights involved in these models are very different and the corresponding reaction rates are also expected to differ widely. As a consequence different reaction pathways may be applicable for reactions taking place in different time frames. (Int J Mass Spectrom 220 (2002) 53–67)

Keywords: Proton-transfer catalysis; Enolization; Ab initio calculations; Dimer radical cation; Potential energy surface

1. Introduction

In the gas phase many small aldehyde and ketone radical cations of low internal energy (i.e., those sampled in the microsecond time-frame) do not undergo isomerization into their enol forms, even though the latter are thermodynamically more stable [1]. The reason for this behavior is that this reaction involves a large barrier [2] as might be expected for a 1,3-H atom shift:

$$RCH_2C(X)O^{\bullet+} \nrightarrow\!\!\!\!\leftrightarrow RCHC(X)OH^{\bullet+}$$

Instead, the radical cation dissociates, e.g., by loosing the X group [3]:

$$RCH_2C(X)O^{\bullet+} \rightarrow RCH_2CO^{+} + X^{\bullet}$$

A case in point is the acetaldehyde radical cation which, in the metastable time-frame, does not rearrange into its more stable enol form, but instead dissociates by loss of an $H^{\bullet}$ atom [4]:

$$CH_3C(H)O^{\bullet+} \rightarrow CH_2C(H)OH^{\bullet+},$$
$$CH_3C(H)O^{\bullet+} \rightarrow CH_3CO^{+} + H^{\bullet}$$

However, recent experimental [3–10] and theoretical studies [11–13] have reported mechanisms by which

* Corresponding author. E-mail: p.j.a.ruttink@chem.uu.nl

1387-3806/02/$ – see front matter
PII S1387-3806(02)00808-4

a gaseous radical cation may rearrange into a more stable isomer through interaction with an appropriate base. One of the earlier examples concerned the isomerization of the methanol radical cation, $CH_3OH^{\bullet+}$, into its more stable ylid isomer $CH_2OH_2^{\bullet+}$ via a 1,2-H shift which is catalyzed by the interaction with a water molecule [5,11], a process termed "proton-transport" catalysis [6]. The catalysis of other 1,2-H shifts have since then been reported [7].

It appeared that 1,3-H shifts (keto to enol transformations) could also be successfully catalyzed by the interaction of a suitable base molecule [3,4,8,10c,10d]. Several mechanisms appeared possible for such catalyzed tautomerizations, as evidenced from the time-honored technique of isotopic labeling [4,8]. Thus, both ionized acetone and acetamide may be induced to rearrange to their more stable enol counterparts via interaction with a base molecule, but the associated mechanisms are quite different. Thus, in the case of acetone, the reaction appears to be a true "proton-transport" catalysis [3], but for acetamide a proton of the "base" molecule appears in the product enol cation [8]:

$$CD_3C(=O)CD_3^{\bullet+} + B\underline{H} \rightarrow CD_2{=}C(OD)CD_3^{\bullet+} + B\underline{H}$$

$$CD_3C(=O)NH_2^{\bullet+} + B\underline{H} \rightarrow CD_2{=}C(O\underline{H})NH_2^{\bullet+} + BD$$

For ionized acetamide, the associated mechanism was traced by ab initio molecular orbital calculations [8].

Prompted by these results we set out to evaluate different reaction path models for catalyzed 1,3-H shifts. These are studied here for the prototype acetaldehyde radical cation, using two catalysts, viz. methanol and acetaldehyde itself ("self-catalysis" [9]). It has recently been shown from ion cyclotron resonance (ICR) experiments that methanol can successfully catalyze the enolization of ionized acetaldehyde [4]; labeling experiments show that this catalyzed isomerization occurs via a direct 1,3-H transfer and not by successive 1,2-H transfers [4].

2. Reaction models

We will consider three models for the catalysis of the H shift in a radical cation:

$$HAB^{\bullet+} \rightarrow ABH^{\bullet+}$$

2.1. Proton-transport catalysis (PTC)

$$HAB^{\bullet+} + M \rightarrow AB^{\bullet} \cdots HM^{+} \rightarrow ABH^{\bullet+} + M$$

In this model the base molecule M abstracts a proton from the radical cation and donates it back to a different site of the incipient radical. In this model one and the same H atom is used in two *proton* shifts. The barriers for the two reactions may be expected to be small (but see below), since a *proton* is shifted instead of a hydrogen *atom*. The catalyst M should satisfy the following condition, where PA is the proton affinity (Radom's PA criterion [12]):

$$PA(AB^{\bullet} \text{ on A}) < PA(M) < PA(AB^{\bullet} \text{ on B})$$

If this condition is met, both proton transfers will be exothermic and successful catalysis may ensue. In addition, the ion–dipole stabilization of the various complexes involved should be sufficiently large to compensate for the activation energies of the two steps. If M is HAB itself then we are dealing with "self-catalysis" (Self-PTC) [9].

2.2. Quid pro Quo (QpQ) [14]

In the above PTC both hydrogen shifts are proton shifts but this does not necessarily mean that these shifts will always proceed without significant activation energies. If for some reason the barrier for the first proton transfer is sufficiently large then an alternative, more economical mechanism may come into play. In this case it is not $HAB^{\bullet+}$ which donates a *proton* to the catalyst, but rather the catalyst donates a hydrogen *atom* to $HAB^{\bullet+}$ to form $HABH^{+}$ which then donates a different hydrogen *atom* back to the incipient radical:

$$HAB^{\bullet+} + \underline{H}R \rightarrow HAB\underline{H}^{+} \cdots R^{\bullet} \rightarrow AB\underline{H}^{\bullet+} + HR$$

In this case both hydrogen shifts are hydrogen *atom* shifts. The following condition must be satisfied:

$$\mathrm{BDE(AH)} < \mathrm{BDE(HR)} < \mathrm{BDE(BH)}$$

where BDE is the bond dissociation energy.

As indicated above by the underlined H, in a QpQ mechanism, a hydrogen of the catalyst appears in the enol product ion and so experimentally a QpQ mechanism may be differentiated from a PTC mechanism by appropriate isotopic labeling [8], with the exception for the PTC case where the catalyst possesses a hydrogen atom that could be interchanged with the accepted proton [4].

The intermediate ions $[HAB–HR]^{\bullet+}$, $[HABH–R]^{\bullet+}$ and $[ABH–HR]^{\bullet+}$ may exist in two forms, as ion–dipole complexes or as distonic ions. In the case of distonic ions the hydrogen shifts corresponds to McLafferty type rearrangements (see Fig. 1) [15]. These two cases behave in the same way with respect to isotopic substitution and so experimentally they give the same mass results. However, the reaction barriers for the two cases will be different and so the two mechanisms may be differentiated computationally. It is also possible that the reaction proceeds according to a mixture of these two forms. As an example of the distonic case see Fig. 1 for the $CH_3CHO^{\bullet+}/CH_3CHO$ combination.

From this figure we see that it is possible to use both the methyl and the aldehyde (–CH=O) hydrogens for the QpQ mechanism. We will indicate the routes followed in Fig. 1a and b by QpQ(CH_3) and QpQ(CH), respectively.

Experimentally, a complication in the QpQ mechanism (and also in the PTC mechanism) may arise if the ionization energy (IE) of HR is close to or smaller than that of HAB. In that case charge exchange may take place prior to reaction to produce ionized $HR^{\bullet+}$ ($HAB^{\bullet+} + HR \rightarrow HAB + HR^{\bullet+}$), followed by the following sequence:

$$HAB + \underline{H}R^{\bullet+} \rightarrow HAB\underline{H}^{+} \cdots R^{\bullet} \rightarrow AB\underline{H}^{\bullet+} + HR$$

In this case the first reaction step corresponds to a *proton* transfer and the second step involves a hydrogen *atom* shift and so $HR^{\bullet+}$ may be considered to act as an “acid”. This sequence of events occurs for the [acetamide/benzonitrile]$^{\bullet+}$ system [8]. Again, if HR is HAB itself then we are dealing with “self-catalysis” (Self-QpQ). In such a case the first step will always be a *proton* transfer.

2.3. Spectator mechanism [11–13]

If the catalyst has a large dipole moment, the TS for the 1,3-H shift in the monomer may be stabilized such that the TS for the complex is lower in energy than the reference combination $HAB^{\bullet+} + M$ at large separation. This TS is an ion–dipole complex of the monomer TS with M or it may be a distonic ion:

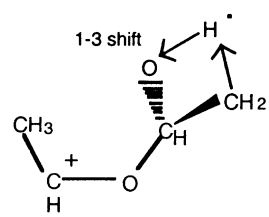

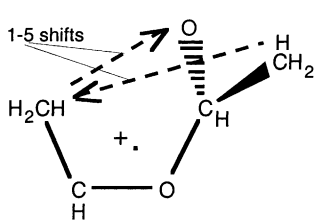

a

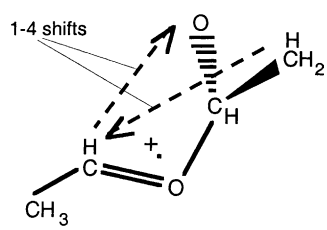

b

Fig. 1. Quid pro Quo mechanisms for self-catalysis of ionized acetaldehyde via distonic intermediates: (a) QpQ(CH_3); (b) QpQ(CH).

3. Theoretical methods

The characterization of the potential energy surface (PES) was started by performing RHF/DZP calculations in order to locate the stationary points for the catalysis models [16]. Single point calculations were performed according to the CBS model for the geometries obtained using RHF/DZP instead of UHF/6-31G(d′), as in the CBS-Q model [17,18]. This method will be denoted by CBS-Q/DZP. In some cases the RHF method leads to intersections of PES's [19] corresponding to different radical site locations. The barrier for the unassisted 1,3-H shift (reaction **TS 1**$^{\bullet+}$–**5**$^{\bullet+}$ in Table 1) is calculated to be 37.1 kcal/mol relative to **1**$^{\bullet+}$ ($CH_3CHO^{\bullet+}$), in excellent agreement with the value obtained by Van der Rest et al., 38.2 kcal/mol [4].

3.1. Self-PTC

For the Self-PTC model a detailed description was given for the analogous acetone case in [9]. For acetaldehyde we also find an intersection of two PES's, corresponding to the radical site either on the O or on the CH_2 group in the $CH_2CHO^{\bullet}\cdots HOCHCH_3^{+}$ complex, leading to a parallel gradient crossing point (PGCP). There also appears to be a TS in the neighborhood of this PGCP. The first step (**TS 6–7**) corresponds to the rate-determining step.

Table 1
Energies for the $CH_3CHO^{\bullet+}/CH_3CHO$ system

Isomer		RHF/DZP (H)	ZPVE (kcal/mol)	CBS-Q/DZP (H)	E_{rel} (kcal/mol)
1	CH_3CHO	−152.95369	37.5	−153.58282	
1$^{\bullet+}$	$CH_3CHO^{\bullet+}$	−152.62428	36.7	−153.20293	0
2$^{\bullet}$	$CH_2CHO^{\bullet}$	−152.32353	28.5	−152.93178	
3$^{\bullet}$	$CH_3CO^{\bullet}$	−152.32891	29.2	−153.94217	
4^{+}	CH_3CHOH^{+}	−153.26907	46.3	−153.87287	
5$^{\bullet+}$	$CH_2CHOH^{\bullet+}$	−152.64522	38.1	−153.22539	−14.1
TS 1$^{\bullet+}$–**5**$^{\bullet+}$		−152.52389	33.8	−153.14387	37.1
5		−152.92985	38.0	−153.56453	
1$^{\bullet+}$ + **1**		−305.57797	74.2	−306.78575	0
2$^{\bullet}$ + **4**$^{+}$		−305.59260	74.8	−306.80465	−11.9
3$^{\bullet}$ + **4**$^{+}$		−305.59798	75.5	−306.81504	−18.4
5$^{\bullet+}$ + **1**		−305.59891	75.6	−306.80821	−14.1
6$^{\bullet+}$		−305.62353	78.2	−306.82375	−23.8
TS 6$^{\bullet+}$–**7**$^{\bullet+}$		−305.57631	72.6	−306.79942	−8.6
7$^{\bullet+}$		−305.58647	76.2	−306.79831	−7.9
TS 7$^{\bullet+}$–**8**$^{\bullet+}$		−305.58476	76.1	−306.79779	−7.6
PGCP 7$^{\bullet+}$–**8**$^{\bullet+}$		−305.58186	–	−306.92031[a]	−17.7[a]
8$^{\bullet+}$		−305.64056	75.8	−306.85472	−43.1
TS 8$^{\bullet+}$–**9**$^{\bullet+}$		−305.63937	73.2	−306.86049	−46.7
9$^{\bullet+}$		−305.64291	76.3	−306.85468	−43.1
Spectator **TS**		−305.52702	75.1	−306.77623	6.0
TS 6$^{\bullet+}$–**10**$^{\bullet+}$		−305.54094	75.0	−306.79361	−4.9
10$^{\bullet+}$		−305.63350	79.0	−306.84852	−39.4
TS 10$^{\bullet+}$–**11**$^{\bullet+}$		−305.55702	73.6	−306.80357	−11.2
11$^{\bullet+}$		−305.62363	76.4	−306.83287	−29.6
12$^{\bullet+}$		−305.61063	74.9	−306.81940	−21.1
TS 12$^{\bullet+}$–**13**$^{\bullet+}$		−305.59695	71.9	−306.84374	−36.4
13$^{\bullet+}$		−305.63667	76.3	−306.85191	−41.5
TS 9$^{\bullet+}$–**13**$^{\bullet+}$		−305.57346	73.6	−306.83272	−29.5

[a] No ZPVE, no crossing on the UHF level, E(electronic, **1**$^{\bullet+}$ + **1**) = −306.89211 H.

3.2. PTC

For the catalysis by methanol (**m**) the situation is slightly different. For the PTC model we again find an intersection of two PES's, corresponding to different radical site localizations in the $CH_2CHO^{\bullet} \cdots H_2OCH_3^{+}$ complex. However, in this case the search for a minimum energy crossing point (MECP) or a PGCP does not succeed, because the intersection terminates at a point with about the same energy as that of the $CH_2{=}CHO^{\bullet} \cdots H_2OCH_3^{+}$ complex (**7m**). We call this the terminal crossing point (TCP). As in the case of a PGCP this implies the existence of a TS in the neighborhood of the TCP. This TS could indeed be located and on the RHF/DZP level it has a slightly lower energy than the TCP. Here too the first step (**TS 6m–7m**) is the rate-determining step.

3.3. QpQ(OH)

The QpQ(OH) model has been described by Van der Rest et al. [4], using MP2/6-31G** calculations for obtaining the stationary points in the PES. However, no TS was found connecting **6m** and **10m** (isomers **3** and **4**, respectively in [4]):

$$CH_3OH \cdots OCHCH_3^{\bullet +} \rightarrow CH_3O^{\bullet} \cdots HOCHCH_3^{+}$$

Although this TS does exist, it turns out to be impossible to connect it properly to the above isomers. The reason is that the PES in this region is discontinuous. For the UHF PES there is an intersection between the PES's corresponding to localization of the radical site on either the methanol or the acetaldehyde moiety for geometries between the TS and **6m**. This leads to a discontinuity in the UHF gradient along the reaction path. For the MP2 PES the situation is even worse, because the space spanned by the occupied MO's is different for the two situations, leading to a discontinuity in the MP2 PES itself. Moreover, the gradients along the reaction path turn out to have different signs. Consequently, a geometry optimization, starting near the transition state geometry does not converge. This situation is depicted schematically in Fig. 2.

Calculations on the RHF/DZP level also lead to an intersection of two PES's. In this case a MECP was found, which then serves as the transition structure for the **6m** to **10m** conversion. Since this intersection also appears to exist on the UHF level, it will exist for any UHF-based correlated method short of full CI. On the other hand, the DFT (B3LYP) method leads to delocalization of the radical site and therefore this method does yield a transition state which may be connected in a continuous manner with the isomers **6m** and **10m**.

4. Results and discussion

For the acetaldehyde$^{\bullet +}$/vinylalcohol$^{\bullet +}$ tautomerization, the PA of the base should lie between 170 and

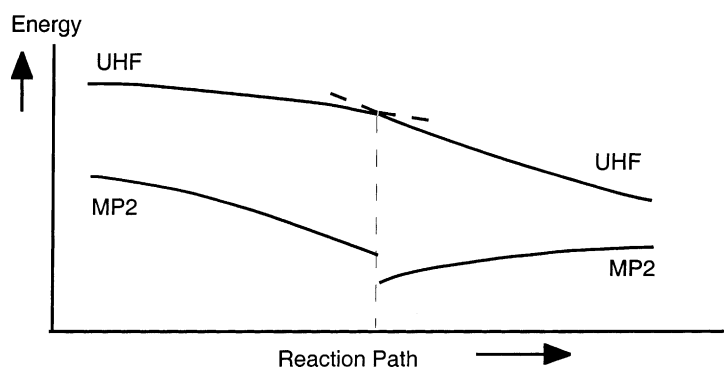

Fig. 2. Schematic UHF and MP2 energy profiles in the neighborhood of the RHF minimum energy crossing point connecting **6m** and **10m**.

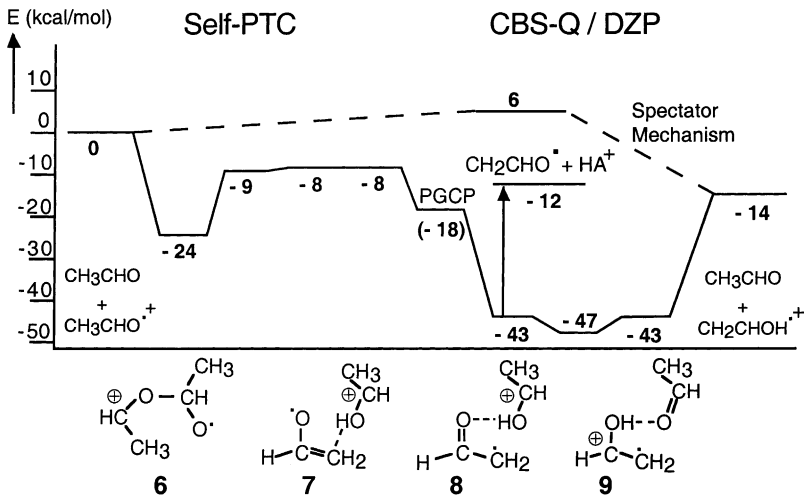

Fig. 3. Energy level diagram for the $CH_3CHO^{\bullet+}/CH_3CHO$ system corresponding to the PTC and Spectator mechanisms.

185 kcal/mol[1] (or between 174 and 189 kcal/mol,[2] or between 172 and 185 kcal/mol (CBS-QB3, this work)) and so acetaldehyde itself, having PA of 184 kcal/mol should be a suitable base ("self-catalysis" [9]).

4.1. Catalysis by acetaldehyde (self-catalysis)

The calculated energies are given in Table 1.

4.1.1. Self-PTC

The reaction proceeds in the same way as for the acetone$^{\bullet+}$/acetone system [9]. The energy level diagram and the structural details of the main structures are given in Fig. 3 and Scheme 1, respectively.

In the search for the TS for the first step, **TS 6–7**, it is important to note that the C_1C_2 bond is much shorter than in ionized acetaldehyde. This situation corresponds to the TS having the radical character on the O, just as in ionized acetaldehyde, with a single (long) C_1O_3 bond and a double (short) C_1C_2 bond. Therefore, the electronic distribution remains more or less undisturbed during this reaction step, which results in a relatively low-lying TS. According to the RHF optimization isomer **7** corresponds to a shallow minimum. Going from **TS 6–7** to **TS 7–8** the neutral moiety undergoes an internal rotation of 130°.

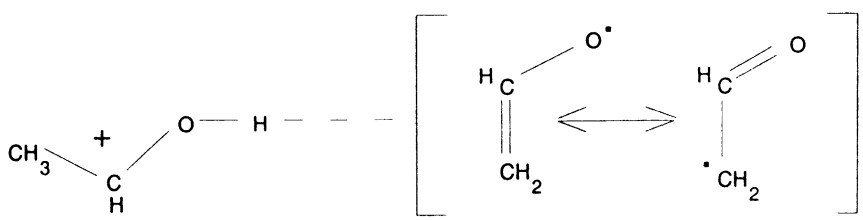

Then after passing the PGCP in the intersection the PES for the $^{\bullet}CH_2CHO\cdots CH_3CHOH^+$ complex is reached. This is an O–H–O bridged structure. According to the RHF electronic energy calculation the H bridge corresponds to a double-minimum potential. However, adding the ZPVE contributions leads to the conclusion that the ground vibrational state is,

[1] Using $\Delta H_f[CH_3C(H)=O]^{\bullet+} = 196$ kcal/mol [1], $\Delta H_f[CH_2=C(H)OH]^{\bullet+} = 181$ kcal/mol [1] and $\Delta H_f[^{\bullet}CH_2C(H)=O] = 0.2$ kcal/mol from [20a].

[2] Using $\Delta H_f[^{\bullet}CH_2C(H)=O] = 4.0$ kcal/mol from [20b].

in fact, delocalized over the two minima. This complex will yield both $^{\bullet}CH_2CHO + CH_3CHOH^+$ and $CH_2CHOH^{\bullet+} + CH_3CHO$.

4.1.2. Self-QpQ

The results are given in Table 1, Scheme 1 and Fig. 4.

For QpQ(CH_3) the initial structure turns out to be the distonic ion **6**. If the CO bond connecting the two moieties remains intact during the isomerization, the H atom shifts correspond to two 1,5 shifts (see Fig. 1a). In this way we find **TS 6–10** connecting **6** with the distonic ion **10**. Going on with **10** we then find a connection to **11**, which dissociates into $CH_3CHO + CH_2CHOH^{\bullet+}$. The rate-determining step (**TS 6–10**) is somewhat higher in energy than for the PTC model, **TS 6–7** (see Fig. 3), but still lower in energy than the starting ions (0 kcal/mol).

In the QpQ(CH) model only ion–dipole complexes are encountered. From the CBS-Q/DZP calculations it appears that the $CH_3CHO\cdots CH_3CHO^{\bullet+}$ complex **12** is unstable with respect to isomerization into the $CH_3CHOH^{\bullet}\cdots OCCH_3^+$ complex **13**. The second H transfer (**13** → **8**/**9**) has a very low-lying TS (at $E_{rel} = -30$ kcal/mol). Consequently, the entire QpQ(CH) reaction in fact corresponds to a one-step mechanism We note that the first step corresponds to a *proton* transfer, whereas the second step corresponds to an H *atom* transfer, as predicted in Section 2.2. Therefore, the role of the two moieties is reversed. Consequently, this is not a catalysis in the strict sense of the term (the "catalyst" is not recovered unchanged after the reaction has taken place).

It is also possible, see Fig. 4, that the intermediate complex **13** dissociates to CH_3CHOH^+ (m/z 45) + $CH_3CO^{\bullet}$; this dissociation limit is calculated to lie 4 kcal/mol below that for the formation of CH_2=$CHOH^{\bullet+}$ (m/z 44) + CH_3CHO. It is therefore expected that enolization will seriously suffer from competition from direct proton transfer, but

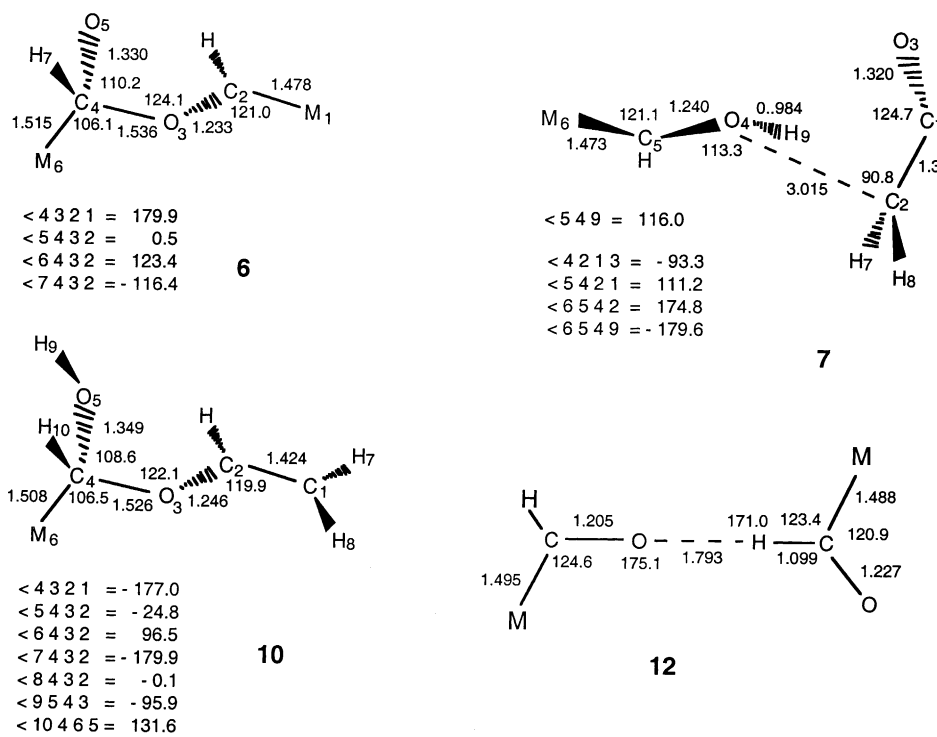

Scheme 1. Geometries of the main structures encountered in the $CH_3CHO^{\bullet+}/CH_3CHO$ potential energy surfaces.

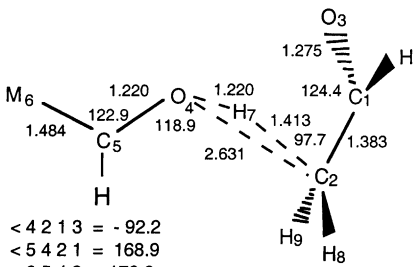

< 4 2 1 3 = - 92.2
< 5 4 2 1 = 168.9
< 6 5 4 2 = 179.9
< 9 2 1 3 = 18.4
< 8 2 1 3 = 160.9

TS 6 - 7

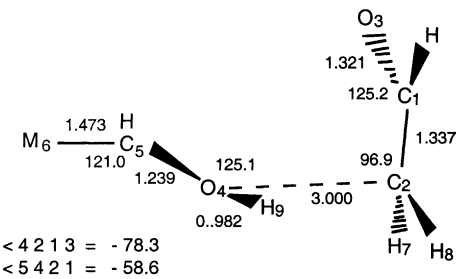

< 4 2 1 3 = - 78.3
< 5 4 2 1 = - 58.6
< 6 5 4 2 = - 175.7
< 6 5 4 9 =
< 7 2 1 3 = 7.7
< 8 2 1 3 = 173.1
< 5 4 6 = 116.7

TS 7 - 8

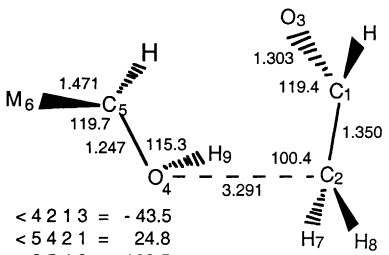

< 4 2 1 3 = - 43.5
< 5 4 2 1 = 24.8
< 6 5 4 2 = 160.5
< 7 2 1 3 = 7.7
< 8 2 1 3 = - 175.6
< 9 4 5 6 = - 178.7
< 5 4 2 = 117.8

PGCP

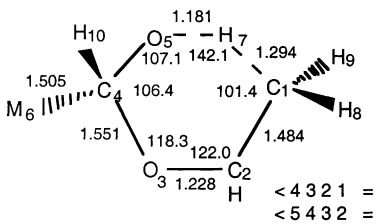

< 4 3 2 1 = - 0.2
< 5 4 3 2 = 36.0
< 6 4 3 2 = 156.1
< 7 1 2 3 = - 16.7
< 7 5 4 3 = - 50.2
< 8 1 2 3 = 98.4
< 9 1 2 3 = - 131.8
< 10 4 6 5 = 132.8

TS 6 - 10

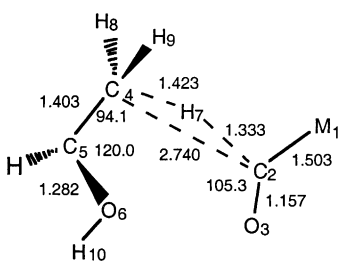

< 7 2 3 = 111.8
< 7 4 5 = 100.1

< 6 5 4 2 = 87.6
< 5 4 2 3 = 9.2
< 1 2 3 4 = 179.3
< 7 4 5 6 = 87.1
< 8 4 5 6 = - 165.8
< 9 4 5 6 = - 18.9
< 10 6 5 4 = 184.4

TS 9 - 13

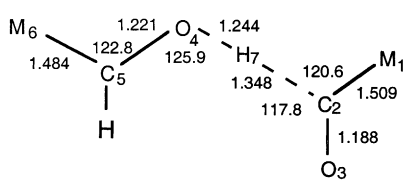

TS 12 - 13

< 2 3 4 = 111.2
< 2 3 5 = 111.2

< 6 1 2 3 = - 103.8
< 5 3 2 1 = 14.0
< 4 3 2 1 = 115.1
< 10 3 2 1 = -112.1
< 8 4 3 5 = 107.4
< 7 4 3 5 = - 101.4
< 9 5 4 3 = - 2.2

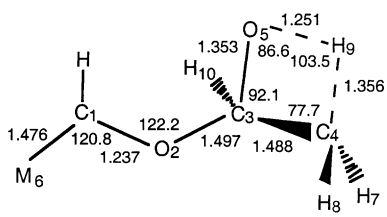

Spectator TS

Scheme 1. (*Continued*).

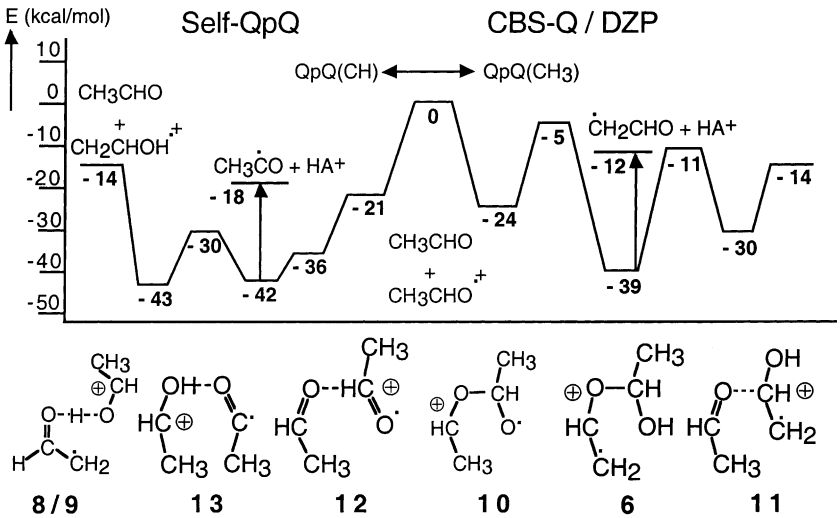

Fig. 4. Energy level diagram for the $CH_3CHO^{\bullet+}/CH_3CHO$ system corresponding to the QpQ mechanism.

since our starting point lies significantly higher, we cannot predict to what extent competition will occur. We can predict however, that if our starting point were to lie below $CH_3CHOH^+ + CH_3CO^\bullet$, i.e., below −18 kcal/mol in Fig. 4, then only CH_3CHOH^+ will be formed. In a previous paper [21] we showed that ionized acetoin, $CH_3C(=O)CH(OH)CH_3^{\bullet+}$ (with $E_{rel} = -26$ kcal/mol, in Fig. 4 [21]) undergoes only one fragmentation in the metastable time-frame, i.e., to $CH_3CHOH^+ + CH_3CO^\bullet$ and that this reaction proceeds via the complex **13**; this shows that ions **13** of low internal energy preferentially undergo direct dissociation.

4.1.3. Spectator mechanism

The optimization of the monomer TS, stabilized by acetaldehyde itself, leads to the distonic form (see above and "Spectator TS" in Scheme 1). Its energy ($E_{rel} = +6$ kcal/mol, see Fig. 3), however, is too high and therefore the Spectator mechanism cannot compete with the PTC and QpQ mechanisms.

4.2. Methanol as the catalyst

The enolization of $CH_3CHO^{\bullet+}$ under the influence of a methanol molecule has been studied by experiment and theory by Audier and coworkers [4]. As argued by these authors methanol has a PA (180 kcal/mol [1]) which lies in the correct range (170–185 kcal/mol [20a], 174–189 kcal/mol [20b], 172–185 kcal/mol (CBS-QB3, this work)).

It was found that the $CH_3CHO^{\bullet+} \cdots CH_3OH$ collision complex undergoes two major reactions, viz. proton transfer to produce $CH_3OH_2^+$ (m/z 33) and formation of the enol ion $CH_2{=}CHOH^{\bullet+}$ (m/z 44) + CH_3OH. These authors' experiments showed that this catalyzed rearrangement occurs via a direct 1,3-H transfer and not by two successive 1,2-H transfers. From ab initio calculations they concluded that the catalysis was better described as a hydrogen atom transport than by a proton transport, pointing towards a QpQ mechanism, see above. Unfortunately, because of isotopic exchange reactions, in the $CH_3CHO^{\bullet+}/CH_3OH$ case no distinction could be made, by labeling experiments, between a PTC and QpQ mechanism.

The calculated energies from our work are given in Table 2.

4.2.1. PTC

The energy level diagram and the structural details of the main structures are given in Fig. 5 and Scheme 2.

Table 2
Energies for the $CH_3CHO^{\bullet+}/CH_3OH$ system (**m**: methanol)

Isomer		RHF/DZP (H)	ZPVE (kcal/mol)	CBS-Q/DZP (H)	E_{rel} (kcal/mol)
1m	CH_3OH	−115.07443	34.6	−115.54042	
1m$^{\bullet+}$	$CH_3OH^{\bullet+}$	−114.71902	32.8	−115.13179	
2m$^{\bullet}$	$CH_3O^{\bullet}$	−114.44787	25.2	−114.87380	8.9
TS 2m$^{\bullet}$**–3m**$^{\bullet}$		−114.35634	22.2	−114.82636	38.6
3m$^{\bullet}$	$CH_2OH^{\bullet}$	−114.44324	25.3	−114.88791	0
4m^{+}	$CH_3OH_2^{+}$	−115.38212	43.1	−115.82443	
5m^{+}	$CH_2OH_2^{\bullet+}$	−114.73245	33.5	−115.56453	
1$^{\bullet+}$ + **1m**		−267.69871	71.3	−268.74335	0
1 + **1m**$^{\bullet+}$		−267.67271	70.3	−268.71461	18.0
2$^{\bullet}$ + **4m**$^{+}$		−267.70565	71.6	−268.75621	−8.1
3$^{\bullet}$ + **4m**$^{+}$		−267.71103	72.3	−268.76660	−14.6
5$^{\bullet+}$ + **1m**		−267.71965	72.7	−268.76581	−14.1
2m$^{\bullet}$ + **4**$^{+}$		−267.71694	71.5	−268.74667	−2.1
3m$^{\bullet}$ + **4**$^{+}$		−267.71231	71.6	−268.76078	−10.9
5 + **5m**$^{\bullet+}$		−267.66230	71.5	−268.71382	18.5
6m$^{\bullet+}$		−267.71870	72.5	−268.76553	−13.9
TS 6m$^{\bullet+}$**–7m**$^{\bullet+}$		−267.69278	69.9	−268.75286	−6.0
7m$^{\bullet+}$		−267.70118	73.4	−268.75167	−5.2
TCP 7m$^{\bullet+}$**–8m**$^{\bullet+}$		−267.69662	–	−268.87123[a]	−16.1[a]
TS 7m$^{\bullet+}$**–8m**$^{\bullet+}$		−267.6995	73.2	−268.76009	−10.5
8m$^{\bullet+}$		−267.75606	72.5	−268.81025	−42.0
TS 8m$^{\bullet+}$**–9m**$^{\bullet+}$		−267.75593	70.9	−268.81391	−44.3
9m$^{\bullet+}$		−267.76019	73.6	−268.81020	−41.9
Spectator **TS**		−267.63618	72.2	−268.72315	12.7
MECP 6m$^{\bullet+}$**–10m**$^{\bullet+}$		−267.70361	–	−268.87058[a]	−15.7[a]
10m$^{\bullet+}$		−267.74799	72.9	−268.78083	−23.5
TS 8m$^{\bullet+}$**–11m**$^{\bullet+}$		−267.66161	70.0	−268.75151	−5.1
TS 10m$^{\bullet+}$**–11m**$^{\bullet+}$		−267.68864	69.2	−268.77600	−20.5
11m$^{\bullet+}$		−267.74751	72.6	−268.79701	−33.7
TS 8m$^{\bullet+}$**–11m**$^{\bullet+}$		−267.68949	71.1	−268.77679	−21.0
TS 11m$^{\bullet+}$**–12m**$^{\bullet+}$		−267.68514	69.9	−268.78345	−25.2
12m$^{\bullet+}$		−267.72725	72.3	−268.77579	−20.4
TS 12m$^{\bullet+}$**–13m**$^{\bullet+}$		−267.71331	69.2	−268.79612	−33.1
13m$^{\bullet+}$		−267.75173	73.3	−268.80590	−39.3

[a] No ZPVE, E(electronic, charge reversed) = −268.86772 H, E(electronic, **1**$^{\bullet+}$ + **1m**) = −268.84564 H.

As explained in [4], the $CH_3CHO^{\bullet+}/CH_3OH$ system satisfies the PA criterion for the PTC model (see Section 2.1). The reaction proceeds along the same lines as for acetaldehyde as catalyst, see above, although the characteristics of the intersection of the PES's for $CH_3OH_2^{+}\cdots CH_2{=}CHO^{\bullet}$ and $CH_3OH_2^{+}\cdots {}^{\bullet}CH_2{-}CH{=}O$ are slightly different (see Section 3.2). The final $AB^{\bullet}\cdots H^{+}\cdots M$ complex will yield both $ABH^{\bullet+}$ and HM^{+}.

4.2.2. QpQ

The results are given in Fig. 6 and Scheme 2. Again we have two possibilities: both the hydroxyl and methyl hydrogens may be used for the shifts. These models are denoted as QpQ(OH) and QpQ(CH_3), respectively.

4.2.2.1. QpQ(OH). The distonic ion $CH_3O(H)^{+}C(H)(CH_3)O^{\bullet}$ appears to be stable.

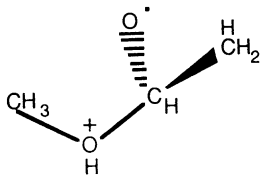

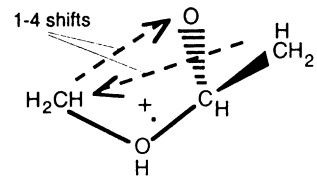

However, this ion is not a good starting point for our reaction, because this reaction would involve 1,3-H atom shifts, which will most likely have high barriers. Instead, we follow the route used by Van der Rest et al. [4]. The CBS-Q/DZP result for the transition point for the conversion of **6m** to **10m** (the MECP in the intersection, see above) indicates that this step has virtually no activation energy. The TS for the second step (**10m** to **8**/**9m**) is 5 kcal/mol more stable than the reference set $CH_3OH + CH_3CHO^{\bullet+}$. Therefore, the QpQ(OH) model is energetically comparable to the PTC model (see Figs. 5 and 6). The reacting configuration for the dissociation is again **8**/**9m**.

4.2.2.2. QpQ(CH_3). As in the QpQ(OH) model we start with the distonic ion $CH_3O(H)^+C(H)(CH_3)O^{\bullet}$. If the distonic structure is preserved, the enolization will correspond to two 1,4-H shifts:

However, the distonic structure is not preserved in the first H transfer. Instead, we find a transition to the ion–dipole complex **6m**. Since this complex very easily converts to **10m** (see above), we are forced to start in the same way as in the QpQ(OH) model. In the latter model a hydrogen from the acetaldehyde methyl group is transferred to the CH_3O oxygen (**10m** to **8**/**9m**). However, it is also possible to transfer the hydroxyl H atom back to the $CH_3O^{\bullet}$ moiety and at the same time transfer an H atom from the incipient methanol moiety to the acetaldehyde oxygen (**TS 10m–11m**). This reaction step may be interpreted as a QpQ mechanism for a catalyzed $CH_3O^{\bullet} \rightarrow CH_2OH^{\bullet}$ isomerization with the CH_3CHOH^+ ion as the catalyst. In the next step an H atom from the CH_3CHOH^+ moiety is transferred to the CH_2 group in the $CH_2OH^{\bullet}$ moiety, leading to the proton-bound $CH_3O(H)\cdots H^+\cdots OCHCH_2^{\bullet}$ complex (**8**/**9m**), which yields either $CH_2CHO^{\bullet} + CH_3OH_2^+$ or $CH_2CHOH^{\bullet+} + CH_3OH$. Starting with **10m** this is a two-step mechanism instead of the one-step mechanism in the QpQ(OH) model. However, both TS's in

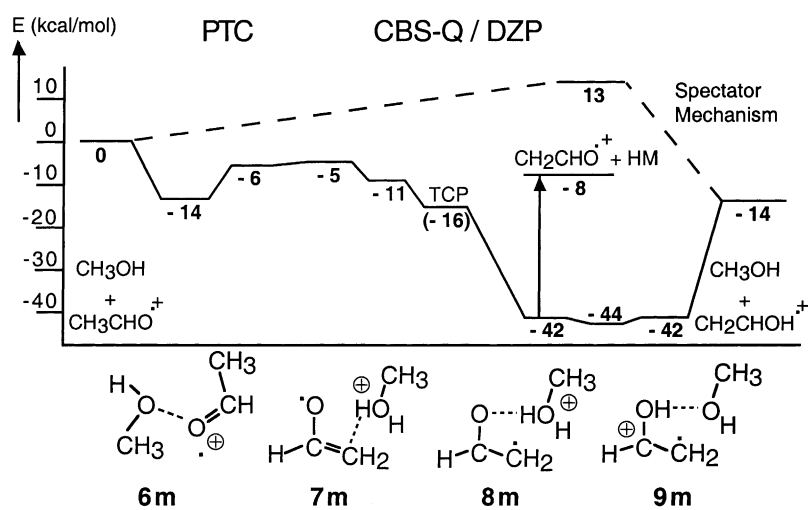

Fig. 5. Energy level diagram for the $CH_3CHO^{\bullet+}/CH_3OH$ system corresponding to the PTC and Spectator mechanisms.

the QpQ(CH_3) model are much lower in energy than the QpQ(OH) TS.

We conclude that the energetically most favorable route to enolization of the acetaldehyde radical cation under the influence of methanol proceeds via the QpQ(CH_3) mechanism.

As is the case with self-catalysis (Section 4.1), for methanol as catalyst too, there is an energetically favorable side reaction. This is the transfer of the CH proton of ionized acetaldehyde to methanol followed by dissociation to $CH_3OH_2^+ + CH_3CO^\bullet$, which lies at the same level as the products of the enolization (−14 kcal/mol). Thus, formation of $CH_3OH_2^+$ should compete with enolization as is indeed observed experimentally [4].

4.2.3. The relationship of the methanol catalyzed tautomerization of ionized acetaldehyde with ionized 1,2-propanediol

The ion–dipole complex $CH_2CHOH^{\bullet+} \cdots CH_3OH$ (**9m**) has been generated and identified independently [22]. The ion is formed by loss of C_2H_4 from ionized 4-methoxybutan-1-ol and is metastable with respect to no less than five fragmentations [22]:

$$\mathbf{9m} \rightarrow CH_3OH_2^+ + CH_3CO^\bullet \quad (m/z\,33)$$

$$\mathbf{9m} \rightarrow CH_3CO^+ + CH_3^\bullet + H_2O \quad (m/z\,43)$$

$$\mathbf{9m} \rightarrow CH_2{=}CHOH^{\bullet+} + CH_3OH \quad (m/z\,44)$$

$$\mathbf{9m} \rightarrow CH_3C(=O)CH_3^{\bullet+} + H_2O \quad (m/z\,58)$$

$$\mathbf{9m} \rightarrow CH_3C(=O)OH_2^+ + CH_3^\bullet \quad (m/z\,61)$$

It was found that at high internal energies (corresponding to an average ion lifetime of ca. 2 μs) the ion dissociates abundantly via direct bond cleavage to its components, $CH_2CHOH^{\bullet+} + CH_3OH$ and to a lesser extent to $CH_3OH_2^+ + C_2H_3O^\bullet$, but that competition of the other three rearrangements becomes prominent at lower internal energies. From a variety of tandem mass spectrometric techniques as well as ab initio calculations it was concluded that prior to dissociation ionized 1,2-propanediol rearranges into same ion–dipole complex **9m** [23], whose heat

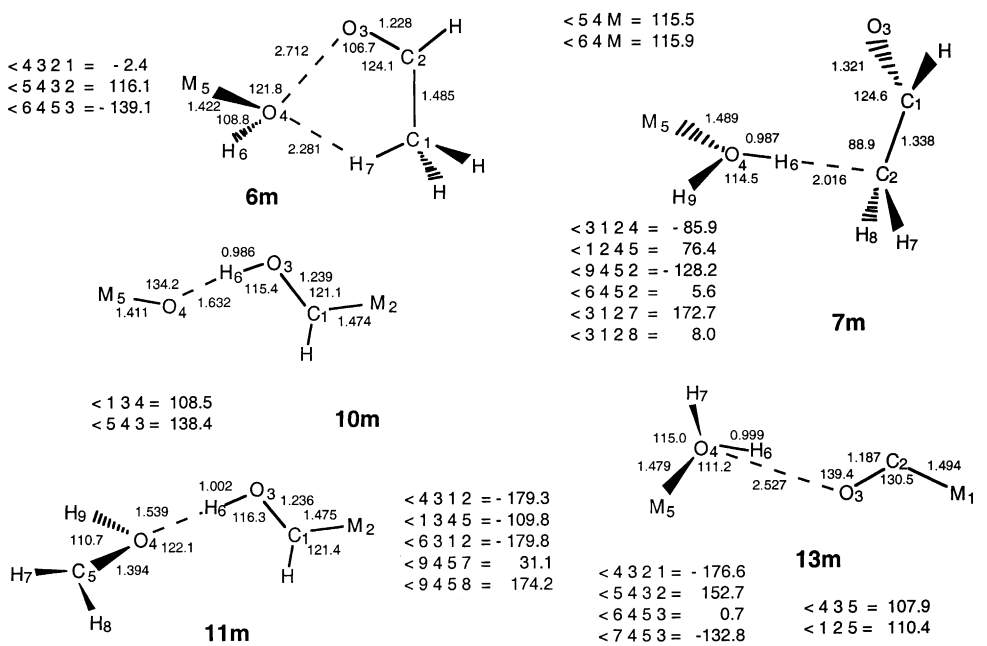

Scheme 2. Geometries of the main structures encountered in the $CH_3CHO^{\bullet+}/CH_3OH$ potential energy surfaces.

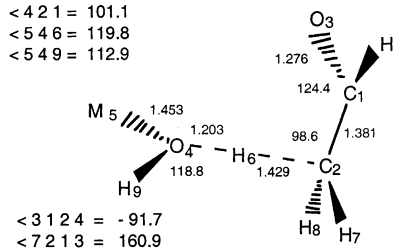

< 4 2 1 = 101.1
< 5 4 6 = 119.8
< 5 4 9 = 112.9

< 3 1 2 4 = - 91.7
< 7 2 1 3 = 160.9
< 8 2 1 3 = 18.4
< 5 4 2 1 = 101.4
< 6 4 5 2 = 3.3
< 9 4 5 2 = - 136.8

TS 6m - 7m

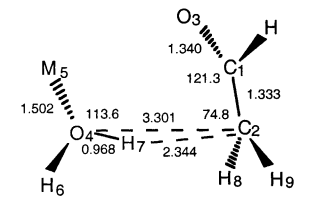

< 4 2 1 3 = - 64.7
< 5 4 2 1 = 81.6
< 6 4 5 2 = - 128.8
< 7 4 5 2 = 7.0
< 8 2 1 3 = 2.8
< 9 2 1 3 = 174.1

< 7 4 5 = 117.0

TS 7m - 8m

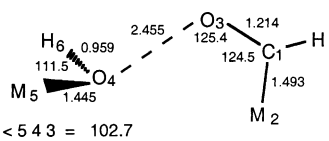

< 5 4 3 = 102.7

< 4 3 1 2 = 1.5
< 5 4 3 1 = 124.0
< 6 4 5 3 = - 74.7

MECP 6m - 10m

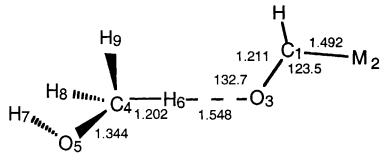

< 4 3 1 2 = 180.0
< 5 4 3 1 = - 141.5
< 6 3 1 2 = 178.6
< 8 4 5 6 = - 112.6
< 9 4 5 6 = 112.5
< 7 5 4 6 = - 84.8

TS 10m - 11m

< 8 4 5 = 114.5
< 9 4 5 = 110.4

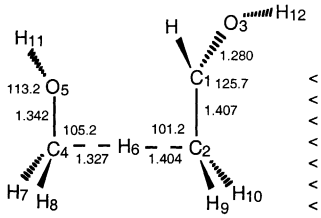

< 2 4 5 = 102.3
< 1 2 4 = 98.6
< 9 2 1 = 115.8
< 10 2 1 = 118.6
< 7 4 5 = 117.4
< 8 4 5 = 112.7
< 6 2 1 4 = 3.5
< 1 2 4 5 = - 2.7
< 4 2 1 3 = - 97.1
< 2 4 5 11 = 106.0
< 9 2 1 4 = - 101.7
< 10 2 1 4 = 113.2
< 7 4 5 2 = - 117.9
< 8 4 5 2 = 104.4
< 12 3 1 2 = - 7.8

TS 8m - 11m

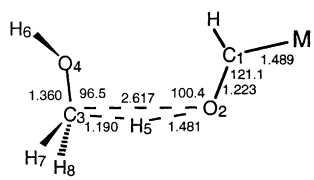

< 3 2 1 M = 182.8
< 1 2 3 4 = - 14.6
< 7 3 4 5 = 115.7
< 8 3 4 5 = - 112.2
< 5 3 4 2 = 6.1
< 6 4 3 5 = - 104.5

TS 11m - 12m

< 4 3 5 = 107.9
< 1 2 5 = 110.4

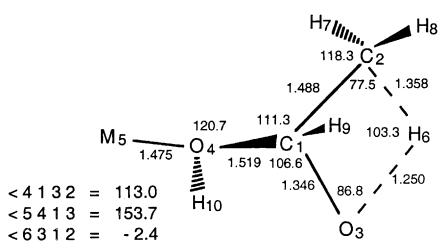

< 4 1 3 2 = 113.0
< 5 4 1 3 = 153.7
< 6 3 1 2 = - 2.4
< 7 2 1 3 = 106.6
< 8 2 1 3 = - 101.3
< 9 1 2 3 = 124.8
< 10 4 5 1 = 135.2

Spectator TS

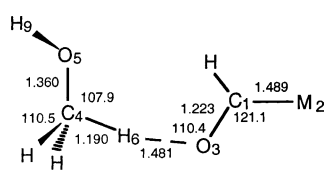

< 4 3 1 2 = 182.8
< 5 4 3 1 = - 14.6
< 6 4 5 3 = 6.1
< 9 5 4 6 = - 104.5

TS 12m - 13m

< 5 4 3 = 96.5
< 1 3 4 = 100.4

Scheme 2. (*Continued*).

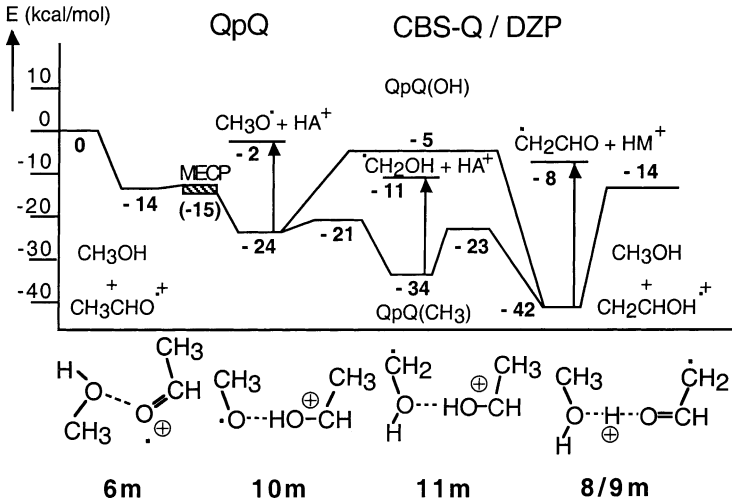

Fig. 6. Energy level diagram for the $CH_3CHO^{\bullet+}$/CH_3OH system corresponding to the QpQ mechanism.

of formation was calculated to lie 32 kcal/mol below the dissociation limit CH_2=$CHOH^{\bullet+}$ + CH_3OH [23b]. The observation that the collision complex $CH_3CHO^{\bullet+} \cdots CH_3OH$, produced in the ICR experiments of Van der Rest et al. [4], produces almost exclusively $CH_2CHOH^{\bullet+}$ and $CH_3OH_2^+$ may be interpreted in terms of the higher starting energy of the collision complex (and consequently larger rate constant for fragmentation) vis-á-vis the internal energy of ion **9m** (see Fig. 5) generated by dissociative ionization. However, attempts to make the collision complex $CH_3CHO^{\bullet+} \cdots CH_3OH$ in a chemical ionization experiment will probably fail because self-protonation of the catalyst ($CH_3OH + CH_3OH^{\bullet+} \rightarrow CH_2OH^{\bullet} + CH_3OH_2^+$) is an exothermic process (by 25 kcal/mol, see Table 2).

5. Conclusions

The PTC and QpQ models may both be used to explain the catalysis of the enolization of acetaldehyde radical cations. For the QpQ model all hydrogens in the catalyst molecule are available for the catalysis. For both catalysts the energetically most favorable reaction route corresponds to transferring the CH hydrogen of the acetaldehyde radical cation to the catalyst. This is a *proton* shift. However, the second step in the Self-QpQ(CH) model (see Fig. 1), corresponds to an H *atom* transfer back to the $CH_3CO^{\bullet}$ moiety. This means that the role of the ion and the molecule in this process is reversed.

We conclude that the most facile way for the acetaldehyde ion to rearrange to its enol form by self-catalysis is via the QpQ(CH) mechanism rather than via a PTC mechanism. It should be possible to differentiate the QpQ mechanisms from the PTC mechanism by isotopic substitution:

PTC : $[CH_3CHO + CD_3CDO]^{\bullet+}$
$\rightarrow CH_2$=$CHOH^{\bullet+}$ (m/z 44)
+ CD_2=$CDOD^{\bullet+}$ (m/z 48)

QpQ : $[CH_3CHO + CD_3CDO]^{\bullet+}$
$\rightarrow CH_2$=$CHOD^{\bullet+}$ (m/z 45)
+ CD_2=$CDOH^{\bullet+}$ (m/z 47)

However, competition from unidirectional proton transfer to produce CH_3CHOD^+ (m/z 46) and CD_3CDOH^+ (m/z 49) may be fierce.

Combining the various reaction models we conclude that

(i) using acetaldehyde as the catalyst may lead to three reactions, viz. $CH_3CHO + CH_2CHOH^{\bullet+}$,

$CH_2CHO^{\bullet}$ + CH_3CHOH^+ and $CH_3CO^{\bullet}$ + CH_3CHOH^+,

(ii) using methanol as the catalyst may lead to five reactions, viz. CH_3OH + $CH_2CHOH^{\bullet+}$, $CH_3O^{\bullet}$+CH_3CHOH^+, $CH_2OH^{\bullet}$+CH_3CHOH^+, $CH_3CO^{\bullet}$ + $CH_3OH_2{}^+$ and $CH_2CHO^{\bullet}$ + $CH_3OH_2{}^+$.

Acknowledgements

MH and PJAR thank The Netherlands Organization for Scientific Research (NWO) for making available the SGI TERAS computer of SARA (Amsterdam).

References

[1] S.G. Lias, J.E. Bartmess, J.F. Liebman, J.L. Holmes, R.D. Levin, W.G. Mallard, J. Phys. Chem. Ref. Data 1 (Suppl. 1) (1988) 17.
[2] (a) F. Turecek, in: Z. Rappoport (Ed.), The Chemistry of Enols, Wiley, Chichester, UK, 1990, p. 95;
(b) Y. Apeloig, in: Z. Rappoport (Ed.), The Chemistry of Enols, Wiley, Chichester, UK, 1990, p. 48.
[3] M.A. Trikoupis, J.K. Terlouw, P.C. Burgers, J. Am. Chem. Soc. 120 (1998) 12131.
[4] G. van der Rest, H. Nedev, J. Chamot-Rooke, P. Mourgues, T.B. McMahon, H.E. Audier, Int. J. Mass Spectrom. 202 (2000) 161.
[5] P. Mourgues, H.E. Audier, D. Leblanc, S. Hammerum, Org. Mass Spectrom. 28 (1993) 1098.
[6] D.K. Bohme, Int. J. Mass Spectrom. Ion Process. 115 (1992) 95.
[7] (a) P.K. Chou, R.L. Smith, L.J. Chyall, H.I. Kenttäma, J. Am. Chem. Soc. 117 (1995) 4374;
(b) H.E. Audier, J. Fossey, P. Mourgues, T.B. McMahon, S. Hammerum, J. Chem. Phys. 100 (1996) 18380;
(c) S.P. de Visser, L.J. de Koning, N.M.M. Nibbering, J. Am. Chem. Soc. 120 (1998) 1517;
(d) M.A. Trikoupis, D.J. Lavorato, J.K. Terlouw, P.J.A. Ruttink, P.C. Burgers, Eur. Mass Spectrom. 5 (1999) 431.
[8] M.A. Trikoupis, P.C. Burgers, P.J.A. Ruttink, J.K. Terlouw, Int. J. Mass Spectrom. 210/211 (2001) 489.
[9] M.A. Trikoupis, P.C. Burgers, P.J.A. Ruttink, J.K. Terlouw, Int. J. Mass Spectrom. 217 (2002) 97.
[10] (a) H.E. Audier, D. Leblanc, P. Audier, T.B. McMahon, S. Hammerum, J. Chem. Soc., Chem. Commun. (1994) 2329;
(b) G. van der Rest, P. Mourgues, J. Tortajada, H.E. Audier, Int. J. Mass Spectrom. 179/180 (1998) 293;
(c) J. Chamot-Rooke, G. van der Rest, P. Mourgues, H.E. Audier, Int. J. Mass Spectrom. 195/196 (2000) 385;
(d) P. Mourgues, J. Chamot-Rooke, G. van der Rest, H. Nedev, H.E. Audier, T.B. McMahon, Int. J. Mass Spectrom. 210/211 (2001) 429.
[11] J.W. Gauld, H.E. Audier, J. Fossey, L. Radom, J. Am. Chem. Soc. 118 (1996) 6299.
[12] J.W. Gauld, L. Radom, J. Am. Chem. Soc. 119 (1997) 9831.
[13] A.J. Chalk, L. Radom, J. Am. Chem. Soc. 121 (1999) 1574.
[14] L.N. Heydorn, P.C. Burgers, P.J.A. Ruttink, J.K. Terlouw, Int. J. Mass Spectrom., in press.
[15] P.J.A. Ruttink, P.C. Burgers, L.M. Fell, J.K. Terlouw, J. Phys. Chem. A 102 (1998) 2976.
[16] (a) M. Dupuis, D. Spangler, J. Wendolowski, NRCC Software Catalogue 1, Program No QG01, GAMESS, 1980;
(b) M. Guest, J. Kendrick, GAMESS User Manual, An Introductory Guide, CCP/86/1, Daresbury Laboratories, 1986.
[17] M.J. Frisch, G.W. Trucks, H.B. Schlegel, G.E. Scuseria, M.A. Robb, J.R. Cheeseman, V.G. Zarzewski, J.A. Montgomery Jr., R.E. Stratman, J.C. Burant, S. Dapprich, J.M. Millam, A.D. Daniels, K.N. Kudin, M.C. Strain, O. Farkas, J. Tomasi, V. Barone, M. Cossi, R. Cammi, B. Mennucci, C. Pomelli, C. Adamo, S. Clifford, J. Ochterski, G.A. Petersson, P.Y. Ayala, Q. Cui, K. Morokuma, D.K. Malick, A.D. Rabuck, K. Raghavachari, J.B. Foresman, J. Ciolowski, J.V. Ortiz, A.G. Baboul, B.B. Stefanov, G. Liu, A. Liashenko, P. Piskorz, I. Komaromi, R. Gomperts, R.L. Martin, D.J. Fox, T. Keith, M.A. Al-Laham, C.Y. Peng, A. Nanayakkara, G. Gonzalez, M. Head-Gordon, E.S. Repogle, J.A. Pople, Gaussian 98, Revision A.9, Gaussian Inc., Pittsburgh, PA, 1998.
[18] (a) J.W. Ochterski, G.A. Petersson, J.A. Montgomery Jr., J. Chem. Phys. 104 (1996) 2598;
(b) J.A. Montgomery Jr., M.J. Frisch, J.W. Ochterski, G.A. Petersson, K. Raghavachari, V.G. Zakrzewski, J. Chem. Phys. 109 (1998) 6505.
[19] P.J.A. Ruttink, P.C. Burgers, Org. Mass Spectrom. 28 (1993) 1087.
[20] (a) J.L. Holmes, F.P. Lossing, J.K. Terlouw, J. Am. Chem. Soc. 108 (1986) 1086;
(b) P.M. Mayer, M.N. Glukhovtsev, J.W. Gauld, L. Radom, J. Am. Chem. Soc. 119 (1997) 12889.
[21] D. Suh, P.C. Burgers, J.K. Terlouw, Int. J. Mass Spectrom. Ion Process. 144 (1995) L1–L7.
[22] J.K. Terlouw, W. Heerma, P.C. Burgers, J.L. Holmes, Can. J. Chem. 62 (1984) 289.
[23] (a) B.L.M. van Baar, P.C. Burgers, J.L. Holmes, J.K. Terlouw, Org. Mass Spectrom. 23 (1988) 355;
(b) P.C. Burgers, L.M. Fell, A. Milliet, M. Rempp, P.J.A. Ruttink, J.K. Terlouw, Int. J. Mass Spectrom. Ion Process. 166/167 (1997) 291.